

See discussions, stats, and author profiles for this publication at: <https://www.researchgate.net/publication/5781579>

Viscoelastic Behavior and In Vivo Release Study of Microgel Dispersions with Inverse Thermoreversible Gelation

ARTICLE *in* BIOMACROMOLECULES · FEBRUARY 2008

Impact Factor: 5.75 · DOI: 10.1021/bm700918d · Source: PubMed

CITATIONS

32

READS

29

6 AUTHORS, INCLUDING:



Jun Zhou

University of Texas at Arlington

119 PUBLICATIONS **1,044** CITATIONS

SEE PROFILE



Liping Tang

University of Texas at Arlington

136 PUBLICATIONS **4,309** CITATIONS

SEE PROFILE

Viscoelastic Behavior and In Vivo Release Study of Microgel Dispersions with Inverse Thermoreversible Gelation

Jun Zhou,[†] Guonan Wang,[†] Ling Zou,[‡] Liping Tang,[‡] Manuel Marquez,^{§, #, ⊥} and Zhibing Hu^{*, †}

Departments of Physics and Materials Science and Engineering, P.O. Box 311427, University of North Texas, Denton, Texas 76203, Department of Bioengineering, University of Texas at Arlington, P.O. Box 19138, Arlington, Texas 76019, NIST Center for Theoretical and Computational Nanosciences, Gaithersburg, Maryland 20899, Harrington Department of Bioengineering, Arizona State University, Tempe, Arizona 85287, and Center for Integrated Nanotechnologies, Los Alamos National Laboratory, Los Alamos, New Mexico 87545

Received August 17, 2007; Revised Manuscript Received October 1, 2007

The dispersion of microgels with two interpenetrating polymer networks of poly(*N*-isopropylacrylamide) and poly(acrylic acid) (PNIPAM-IPN-PAAC) has been studied for its viscoelastic behavior, biocompatibility, and in vivo release properties. The IPN microgels in water had an average hydrodynamic radius of about 85 nm at 21 °C, measured by dynamic light scattering method. The atomic force microscope image showed that the particles were much smaller after they were dried but remained spherical shape. The storage and loss moduli (G' and G'') of dispersions of IPN microgels were measured in the linear stress regime as functions of temperature and frequency at various polymer concentrations using a stress-controlled rheometer. For dispersions with polymer concentrations of 3.0 and 6.0 wt % above 33 °C, the samples behave as viscoelastic solids and the storage modulus was larger than the loss modulus over the entire frequency range. The loss tangent was measured at various frequencies as a function of temperature. The gelation temperature was determined to be 33 °C at the point where a frequency-independent value of the loss tangent was first observed. At pH 2.5, when heated above the gelation temperature, IPN microgels flocculate by pumping a large amount of water from the gel. When the pH value was adjusted to neutral, deprotonation of $-\text{COOH}$ groups on PAAC made the microgel keep water even above the gelation temperature. Using an animal implantation model, the biocompatibility and drug release properties of the IPN microgel dispersion were evaluated. Fluorescein as a model drug was mixed into an aqueous microgel dispersion at ambient temperature. This drug-loaded liquid was then injected subcutaneously in Balb/C mice from Taconic Farms. The test results have shown that the IPN microgels did not adversely promote foreign body reactions in this acute implantation model and the presence of gelled microgel dispersion substantially slowed the release of fluorescein.

Introduction

Poly(*N*-isopropylacrylamide) polymer and its derivatives have been studied extensively because they exhibit a sharp thermoreversible phase transition and easily accessible, tunable lower critical solution temperature (LCST) near physiological temperature.^{1–4} Copolymers of *N*-isopropylacrylamide (NIPAAm) and poly(acrylic acid) (PAAC) have been prepared using the reversible addition–fragmentation chain transfer (RAFT) polymerization method, and they are useful in a variety of molecular switching and drug delivery applications where responses to small pH changes are relevant.⁵ Injectable copolymers of PNIPAAm-co-AAc⁶ and PNIPAM-co-AAc hydrogel scaffolds with proteolytic degradability by incorporation of an oligopeptide cross-linker⁷ were prepared for biomedical applications. Intramolecular complex formation of PNIPAM with human serum albumin was investigated for enhancing understanding of the mechanisms of biomacromolecular interactions available in nature.⁸

Recently, we have developed microgels consisting of polymer interpenetrating networks (IPN) of PNIPAM and PAAC (PNIPAM-IPN-PAAC).^{9–12} One of the major advantages of the PNIPAM-IPN-PAAC over the copolymers of PNIPAM-co-PAAC is that the phase transition temperature of the PNIPAM remains the same, while the random copolymerization results in the increasing LCST of the system upon the increase of PAAC.³ Even more unusual, we have found that aqueous dispersion of PNIPAM-IPN-PAAC microgels can transfer from a liquid at room temperature to a physically bonded microgel network above 33 °C.^{9,10} Many polymeric systems can form gels via normal thermoreversible sol–gel transitions without chemical cross-linking such as gelatin and polysaccharides,^{13,14} which are a liquid at a higher temperature and become a gel at an lower temperature. Some polymeric solutions have an inverse thermoreversible gelation including poly(ethylene oxide)-poly(propylene oxide)-poly(ethylene oxide) triblock copolymers (Pluronic or Poloxamer)¹⁵ and degradable triblock copolymers.¹⁶ However, there are few reports on microgels dispersions that undergo an inverse thermoreversible gelation.

In this paper, we report the study of viscoelastic behavior and controlled release in vivo of the PNIPAM-IPN-PAAC microgel dispersion. Viscoelastic behavior is one of the most important properties of colloidal or polymer dispersions and

* Corresponding author. E-mail: zbhu@unt.edu.

[†] University of North Texas.

[‡] University of Texas at Arlington.

[§] NIST Center for Theoretical and Computational Nanosciences.

[#] Arizona State University.

[⊥] Los Alamos National Laboratory.

related to biomacromolecule applications.^{17,18} Previously, viscoelastic behavior of concentrated colloidal dispersions of a core-shell latex have been studied.¹⁹ It is found that by chemically fixing a thermosensitive PNIPAM shell onto the surface of a charge-stabilized PS core, the rheological properties of which can be controlled by temperature.¹⁹ On the other hand, rheological behavior of spherical PNIPAM microgels were investigated.²⁰ The dispersion of these microgels are liquid but becomes physically close-packed above the LCST of the PNIPAM.²⁰ The dispersion of PNIPAM-IPN-PAAC microgels studied here should be a good model system for investigations of the inverse thermoreversible gelation. The biocompatibility and controlled release properties of the IPN microgel dispersion have also been studied in the subcutaneous cavity of mice.

Experimental Section

Materials. *N*-Isopropylacrylamide was purchased from Polysciences, Inc. Dodecyl sulfate sodium salt 98%, potassium persulfate, acrylic acid 99%, *N,N'*-methylenebisacrylamide 99%, tetramethylethylenediamine, and ammonium persulfate were purchased from Aldrich. Distilled and deionized water was used through all the experiments.

IPN Microgel Preparation. PNIPAM-IPN-PAAC microgels were synthesized according to previous reports.^{9,10} First, we prepared PNIPAM microgels using precipitation polymerization. *N*-Isopropylacrylamide (3.8 g), 0.07 g of *N,N'*-methylenebisacrylamide, and 0.6 g of sodium dodecyl sulfate were dissolved in 240 g of distilled and deionized water under continuous stirring for 1 h. After the solution was bubbled for 40 min at 70 °C using nitrogen gas, 0.166 g of potassium persulfate was dissolved in 20 mL of DI water and added to start the polymerization. The reaction lasted for 4 h at 70 °C under nitrogen atmosphere. The PNIPAM microgels were then dialyzed (Spectra/Por 7 dialysis membrane, MWCO 14000, VWR) against DI water for two weeks at room temperature to remove the unreacted monomers and surfactant. The final PNIPAM microgel concentration was adjusted to 13 mg/mL.

Second, we used PNIPAM microgels as seeds to prepare PNIPAM-IPN-PAAC microgels. The as-prepared PNIPAM microgel-solution (35 g) was diluted to 350 g with DI water. *N,N'*-Methylenebisacrylamide (0.5 g) and 2.3 g of acrylic acid were added. The solution was stirred for 120 min at 22 °C with nitrogen gas purging. Ammonium persulfate (0.2 g) and 0.2 g of tetramethylethylenediamine separately dissolved in 10 g of DI water were added rapidly to the solution. The reaction mixture was kept at 22 °C for 40 min under nitrogen atmosphere. The obtained PNIPAM-IPN-PAAC microgels were purified through dialysis. The weight ratio of PNIPAM to PAAC within the IPN microgels was 1:0.20, determined by the evaporation method. The composition of PAAC and PNIPAM within the IPN was calculated as follows: First, we obtained the dried weight (W_{NIPAM}) of PNIPAM microgels in the dispersion. The same weighted PNIPAM microgels were used for IPN microgels. The resultant IPN microgels were then dried and weighted to obtain W_{IPN} . The weight percentage of the PNIPAM in the IPN microgel was determined by $W_{\text{NIPAM}}/W_{\text{IPN}} \times 100\%$ and of the PAAC by $(1 - W_{\text{NIPAM}}/W_{\text{IPN}}) \times 100\%$.

Particle Size Measurements. The sizes of PNIPAM and IPN microgels in water were measured using a dynamic light scattering spectrometer (ALV, Germany), which was equipped with an ALV-5000 digital time correlator and a helium-neon laser (Uniphase 1145P, output power of 22 mW and wavelength of 632.8 nm). All the measurements were carried out at a scattering angle of 90°. The sample temperature was controlled with a refrigerator circulating water bath.

Rheological Characterization. Dynamic rheological analysis was performed with a stress-controlled rheometer (ATS Viscoanalyser) equipped with a solvent trap to prevent water evaporation. The parallel plate geometry with the plate diameter of 25 cm was used, and the sample gap was adjusted to 0.5 mm. All the rheological experiments were performed within the linear viscoelastic region. The results were analyzed with Rheoexplorer v5.0 software.

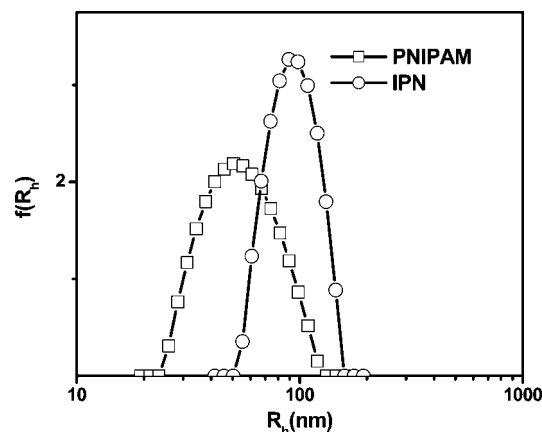


Figure 1. Distribution of hydrodynamic radius of PNIPAM and IPN microgels at 21 °C. The polymer concentration of the PNIPAM and IPN microgel dispersions were the same as 5.0×10^{-6} g/mL with pH 7.

Atomic Force Microscopy (AFM). The AFM image was obtained with a Veeco/Digital Instruments Nanoscope III AFM operating in tapping mode with a drive frequency of 270 kHz. Samples were prepared by casting 4–5 drops of dispersion onto a glass slide, and they were allowed to dry.

In Vivo Testing. Animal implantation model was used to determine the biocompatibility and drug slow release properties of PNIPAM-IPN-PAAC microgel dispersion. Briefly, fluorescein, as a model drug (with final concentration of 0.04%), was added into an aqueous dispersion of PNIPAM-IPN-PAAC microgels with a polymer concentration of 6 wt % at ambient temperature. Because the microgel dispersion is a free-flowing liquid, fluorescein can be uniformly mixed with the dispersion under stirring. This drug-loaded liquid was then injected subcutaneously in Balb/C mice (25 g body weight) from Taconic Farms (Germantown, NY). After implantation for 24 h, implant-bearing mice were sacrificed and the implants and the surrounding tissues were then frozen in OCT embedding media (Polysciences Inc., Warrington, PA) at −80 °C. Sections 10 μ m thick were sliced using a Leica cryostat (CM1850) and placed on poly(L-lysine) coated slides. To assess the tissue responses to microgel implants, some of these slides were H&E stained. To determine the amount of residual fluorescein, the slide sections were observed using a Leica fluorescence microscope (Leica Microsystems) equipped with a Nikon E500 Camera (8.4 V, 0.9 A, Nikon Corporation, Japan).

Results and Discussion

A. Characterization of IPN Microgels. Figure 1 shows the size distributions of hydrodynamic radii of PNIPAM and IPN microgels at 21 °C. The polymer concentration of the PNIPAM and IPN microgel dispersions were the same as 5.0×10^{-6} g/mL at pH 7. The radius of the IPN microgel is larger than the one for PNIPAM microgel because of the addition of hydrophilic PAAC polymer network, making the microgel absorb more water at room temperature. Because a large amount of surfactant was used to produce these smaller PNIPAM particles, their size distribution was broader than larger particles. The secondary PAA network may restrict the extension of tangling chains or blobs in these PNIPAM microgel surfaces. As a result, the size of IPN microgels appears more uniform.

The atomic force microscope image and its enlargement of the IPN microgels are presented in Figure 2. Comparing with dynamic light scattering spectrum in Figure 1, one can see that the average particle diameter of microgels is reduced considerably to about 50 nm in the AFM image. This is because the microgels were dried for AFM measurements while they were

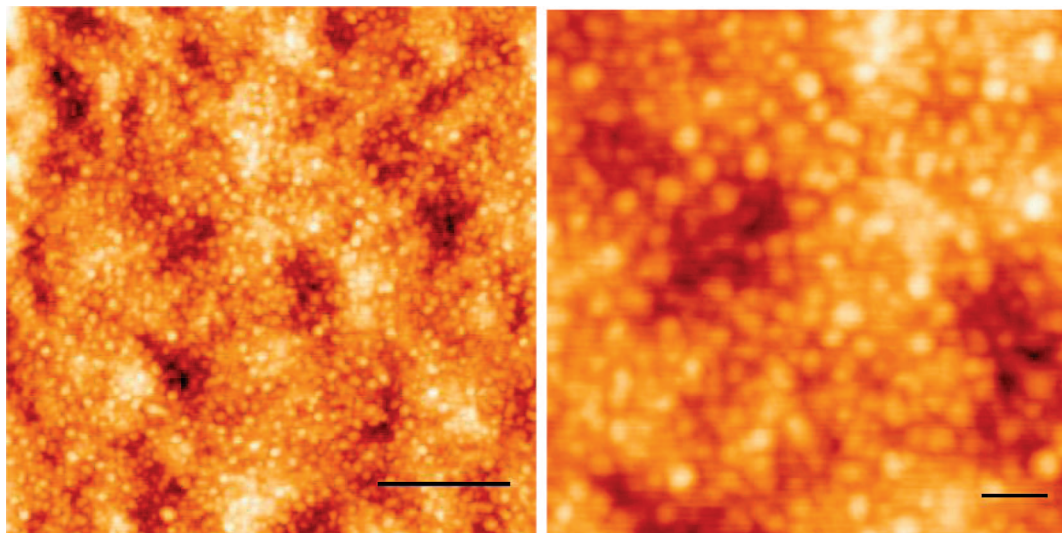


Figure 2. AFM image (left) and its enlargement (right) of PNIPAM-IPN-PAAc microgels. The microgels were dried after the IPN dispersion was cast in a glass slide. The scale bars are 0.5 (left) and 0.1 (right) μm , respectively.

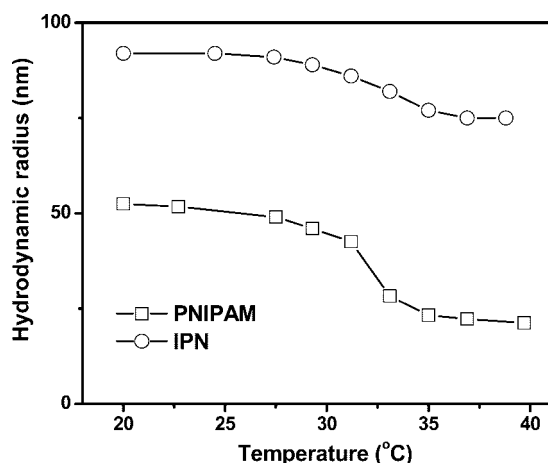


Figure 3. Temperature dependence of hydrodynamic radii for the diluted PNIPAM and IPN microgel dispersions at pH 7.

swollen in water for light scattering measurements. As shown in Figure 2, although the size of microgels was reduced during the drying process, the particles remained in a spherical shape.

Figure 3 shows temperature-induced volume phase transition. The IPN microgel undergoes a volume phase transition at 33 °C that is the same as the one for the PNIPAM microgel. For a randomly copolymerized PAAc/PNIPAM gel, the volume phase transition temperature increases with PAAc concentration.³ The volume change of the IPN microgel below and above the volume transition temperature is smaller than that of the PNIPAM. This is because the PAAc network in the IPN is not sensitive to the temperature change and can reduce the shrinkage of the PNIPAM network.

B. Viscoelastic Behavior of the IPN Microgel Dispersions.

To ensure that the rheological measurements were performed within linear viscoelastic region, a stress sweep experiment at a frequency of 0.1 Hz was carried out to define this region from 20 to 40 °C. Figure 4 shows a typical stress dependence of storage and loss modulus, G' and G'' , respectively, of the dispersions of PNIPAM-IPN-PAAc microgels at 37 °C, where there is no significant change in G' and G'' below 10 Pa. To avoid possible stress induced sliding between the microgels²⁰ and obtain good signals, we have used the stress of 2 Pa for all the data taken by the rheometer.

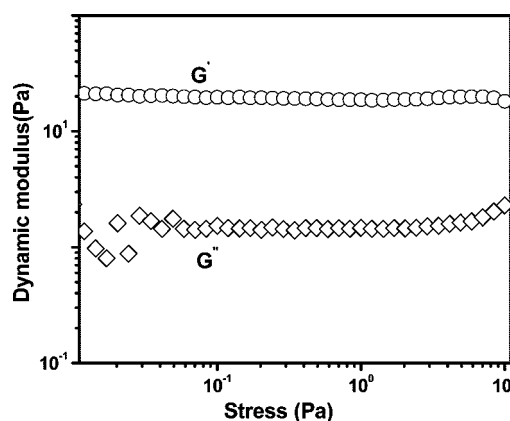


Figure 4. Stress dependence of storage and loss moduli (G' and G'') of the dispersion of IPN microgels at 37 °C. The polymer concentration of the dispersion is 3.0 wt %.

The storage and loss moduli G' and G'' of dispersions of IPN microgels are shown in Figure 5 as a function of temperature at various polymer concentrations. At a low polymer concentration of 1.5 wt %, G'' is always larger than G' over the entire temperature range studied. This indicates that the dispersion remains in a liquid state. When the temperature increases from 25 to 32 °C, both G' and G'' decrease with the temperature increase. This is the common behavior of a polymer solution.^{21–23} For polymer solutions, dynamic modulus decrease can be ascribed to increase in chain flexibility and compactness of polymer molecules in solution with increasing temperature. However, for our samples that consist of the microgels dispersed in the water, the decrease in the dynamic modulus can result from the decrease of particle size and hydrogen-bonded hydration water with increasing temperature. When temperatures further increase, both G' and G'' increase sharply, and the growth rate of G' is much more than that of G'' . This indicates that there are interactions among microgels upon the temperature increases above 33 °C. However, these interactions are not large enough to make the fluid to become a gel at this low polymer concentration.

As polymer concentration increases from 1.5 to 3.0 wt %, there is an interception between G' and G'' at 33 °C (Figure 5b). Below this temperature, G'' is larger than G' , but above it, G' has much higher values than G'' . This indicates that the elastic

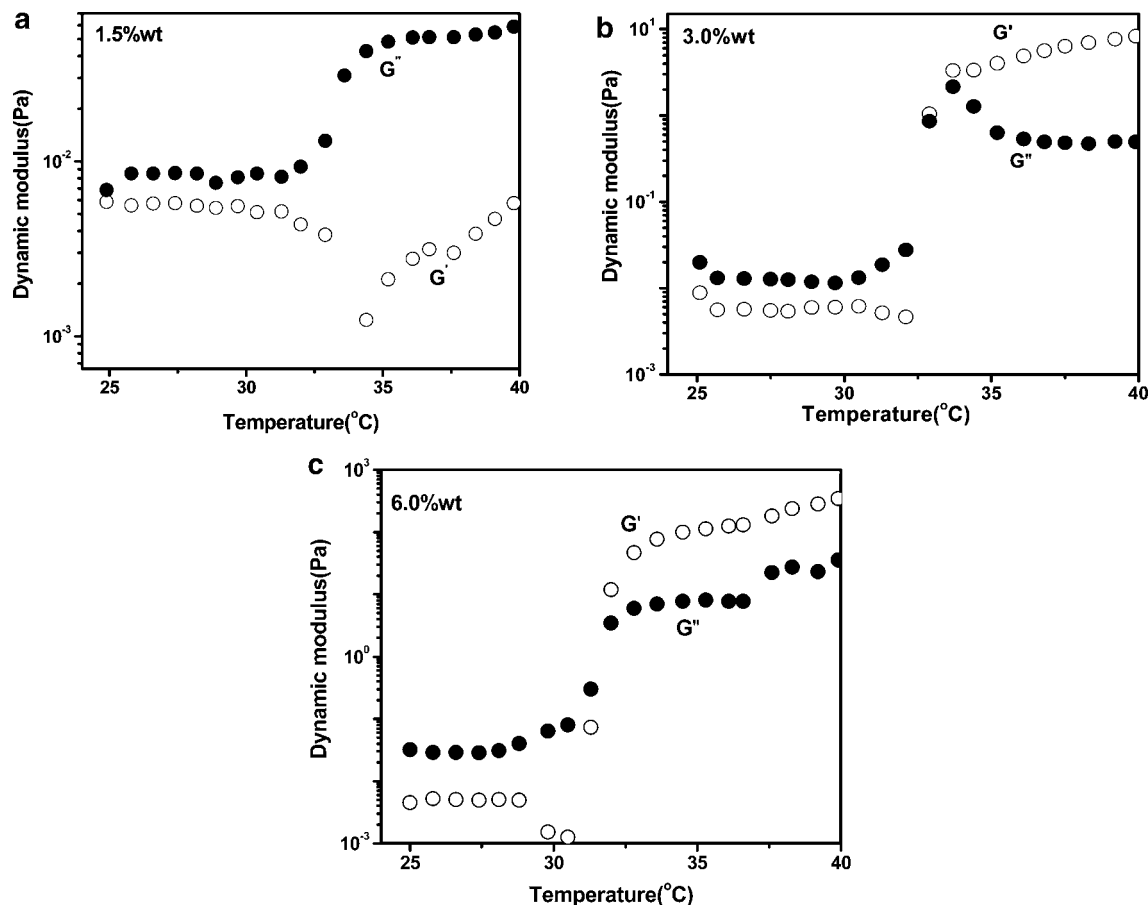


Figure 5. Evolution of dynamic modulus of PNIPAM-IPN-PAAc microgels (pH 7) with temperature increase at different polymer concentrations: (a) 1.5, (b) 3.0, and (c) 6.0 wt %, respectively.

response dominates due to the formation of the physical network of IPN microgels. For a higher polymer concentration of 6 wt %, the interception point remains the same as one as for the 3.0 wt % sample (Figure 5c).

The frequency dependence of storage and loss moduli, G' and G'' , respectively, was determined in low-amplitude oscillatory shear experiments, as shown in Figure 6a for IPN microgel dispersions at polymer concentration of 3.0 wt % for three different temperatures. At 34 and 37 °C, the samples behave as viscoelastic solids and the storage modulus is larger than the loss modulus over the entire frequency range. G' is independent of frequency and corresponds to the plateau modulus, G_p . G_p at 37 °C is higher than G_p at 34 °C. This indicates that the physical gel of the microgels becomes mechanically stronger as the temperature is increased higher above 33 °C. Figure 6b showed frequency dependency of G' and G'' for the IPN with different concentrations at 37 °C. For 1.5 wt % dispersion, G' was less than G'' and both G' and G'' depended on frequency. This is a typical viscoelastic solution behavior.¹⁸ However, when the concentration of IPN increases to 3.0 and 6.0 wt %, G' was larger than G'' and frequency independency of G' and G'' was observed, which is characteristic of a solidlike state.

To determine the gelation temperature, we have used Winter and Chambon's method²⁴ by measuring loss tangent ($\tan(\delta) = G''/G'$) at various frequencies, as shown in Figure 7 for IPN microgel dispersion at polymer concentration of 3 wt % with stress of 2 Pa. It can be seen from Figure 7 that the loss tangent is frequency dependent and decreases during the gel formation, indicating that the dispersion becomes more and more elastic.

The gelation temperature is identified at the point where a frequency-independent value of the loss tangent is first observed.^{24,25} We thus determined that the gelation temperature for our system is 33 °C for our sample.

It is noted this gelation temperature is the same as the volume phase transition temperature (VPTT) for the PNIPAM microgels. The VPTT is determined by the sharpest change in the particle radius, as shown in Figure 3. Above the VPTT, the PNIPAM microgels change from a hydrophilic swelling state to a hydrophobic collapsed state. We thus conclude that the connectivity among microgels during the gelation was provided by hydrophobic interactions among the microgels. In contrast to pure PNIPAM microgels that shrink above the VPTT, the PNIPAM-IPN-PAAc microgels do not shrink significantly due to the mechanical support from nonshrinking PAAc component of the IPN. As a result, microgels can interact with each other in a close distance via hydrophobic interaction to form a gel.

Because PAAc within PNIPAM-IPN-PAAc microgels is weak acid ($pK_a \approx 4.30$), it is expected that the gelation of IPN microgel dispersions depends on pH value effect. At pH 2.5, the protonation of carboxylic group within PAAc weakens the ability to absorb water. Complexation due to hydrogen bonding between $-\text{COOH}$ groups on PAAc and $-\text{CONH}-$ groups on PNIPAM repels water out from IPN microgels. More important, complex formation makes IPN microgels more hydrophobic. Therefore, when heated above the VPTT, due to the increase of hydrophobic interaction and lack of electrostatic repulsion between IPN microgels, IPN microgels flocculate by pumping a large amount of water from the gel, as shown in Figure 8a. It had been reported that PNIPAM-*co*-vinyl laurate microgels

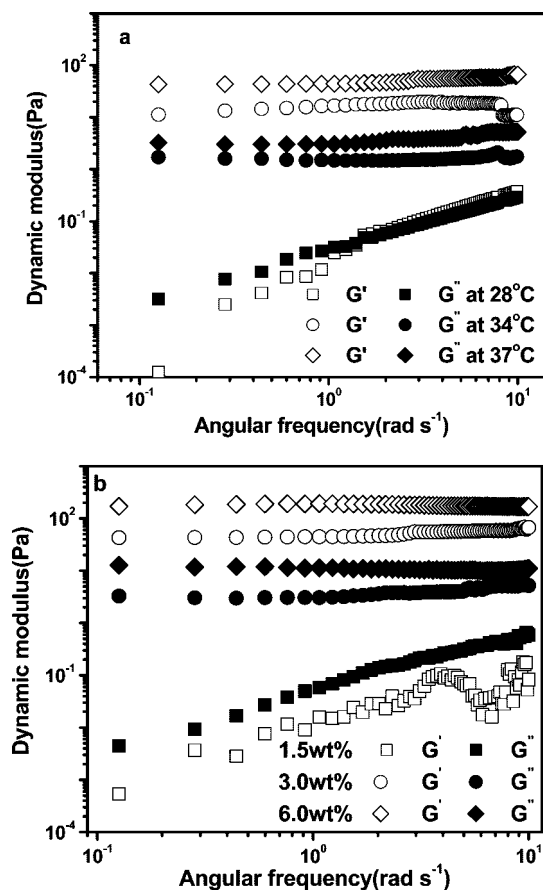


Figure 6. Storage modulus, G' , and loss modulus, G'' , as a function of angular frequency (ω). (a) varying the temperature: 28, 34, and 37 °C, while the polymer concentration remains the same at 3.0 wt %. (b) varying the polymer concentration: 1.5, 3.0, and 6.0 wt %, while the temperature remains the same at 37 °C.

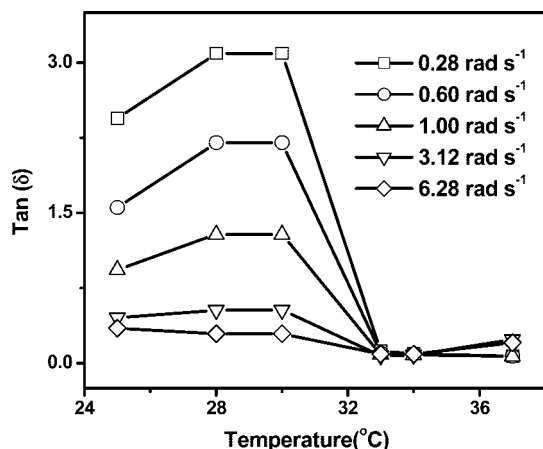


Figure 7. Temperature dependence of loss tangent ($\tan(\delta) = G''/G'$) at various oscillatory frequencies of 0.28, 0.60, 1.0, 3.12, and 6.28 rad/s. The stress applied is 2 Pa and the polymer concentration of IPN microgel dispersion is 3.0 wt % at pH 7.

undertook an irreversible gelation upon heating due to the existence of hydrophobic vinyl laurate.²⁶ It is noted that, in our case, the inverse gelation was reversible even at pH 2.5.

When the pH value was adjusted to neutral, deprotonation of $-\text{COOH}$ groups on PAAc breaks complex structures between PAAc and PNIPAM and makes the microgel keep water even above the gelation temperature. At the same time, ionic charges on PAAc are temperature-independent and prevent the collapse of the particles into an aggregate, as seen in Figure 8b. Indeed,

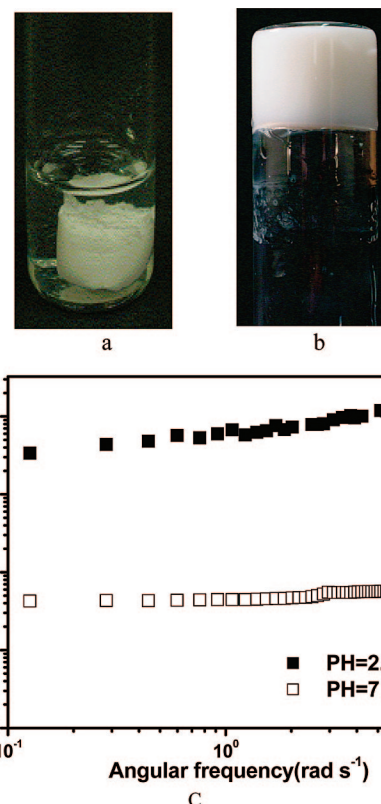


Figure 8. pH effect on the gelation behavior. The polymer concentration of the dispersion of PNIPAM-IPN-PAAC microgels is 3.0 wt % and the temperature is at 37 °C: (a) Gelation at pH 2.5 (water was pumped out from the gel). (b) Gelation at pH 7.0 (no water was pumped out from the gel). (c) Frequency dependence of storage moduli for IPN microgel dispersion 37 °C at pH 2.5 and pH 7, respectively.

we observed that no water was expelled after the IPN microgel dispersion at pH 7 was kept at 37 °C for one week. Figure 8c shows frequency dependence of storage moduli (G') of IPN microgels network at 37 °C at pH 2.5, and pH 7, respectively. G' at pH 2.5 is much larger than one at pH 7. This again demonstrates that the solid content of the gel at pH 2.5 (less water) is more than that at pH 7.0.

C. Biocompatibility and In Vivo Drug Release Experiments. Via an animal implantation model,^{12,27} we have observed that PNIPAM-IPN-PAAC microgels show mild accumulation of the inflammatory cells inside and surrounding implants similar to PNIPAM particles and better than poly(L-lactic acid) particles and polystyrene particles found in our recent study.²⁷ In this study, we further relate the biocompatibility study with controlled release in vivo of PNIPAM-IPN-PAAC microgels. This is because one of the most interesting applications of microgels dispersions with thermal gelling capabilities may be in the area of controlled drug release.

The loading of the microgel dispersion with a drug has been achieved by simple mixing of the drug with already-prepared dispersion. After subcutaneous implantation in mice, this liquid quickly gelled inside animals because the mice body temperature (~ 37 °C) was higher than the gelation temperature of 33 °C, as revealed by viscoelastic study above. After implantation for 24 h, the biocompatibility and drug slow release characteristics of PNIPAM-IPN-PAAC microgel were evaluated.

H&E stain of the implants show mild accumulation of the inflammatory cells inside and surrounding implants by compared with saline control (Figure 9a,b). By injecting fluorescein alone,

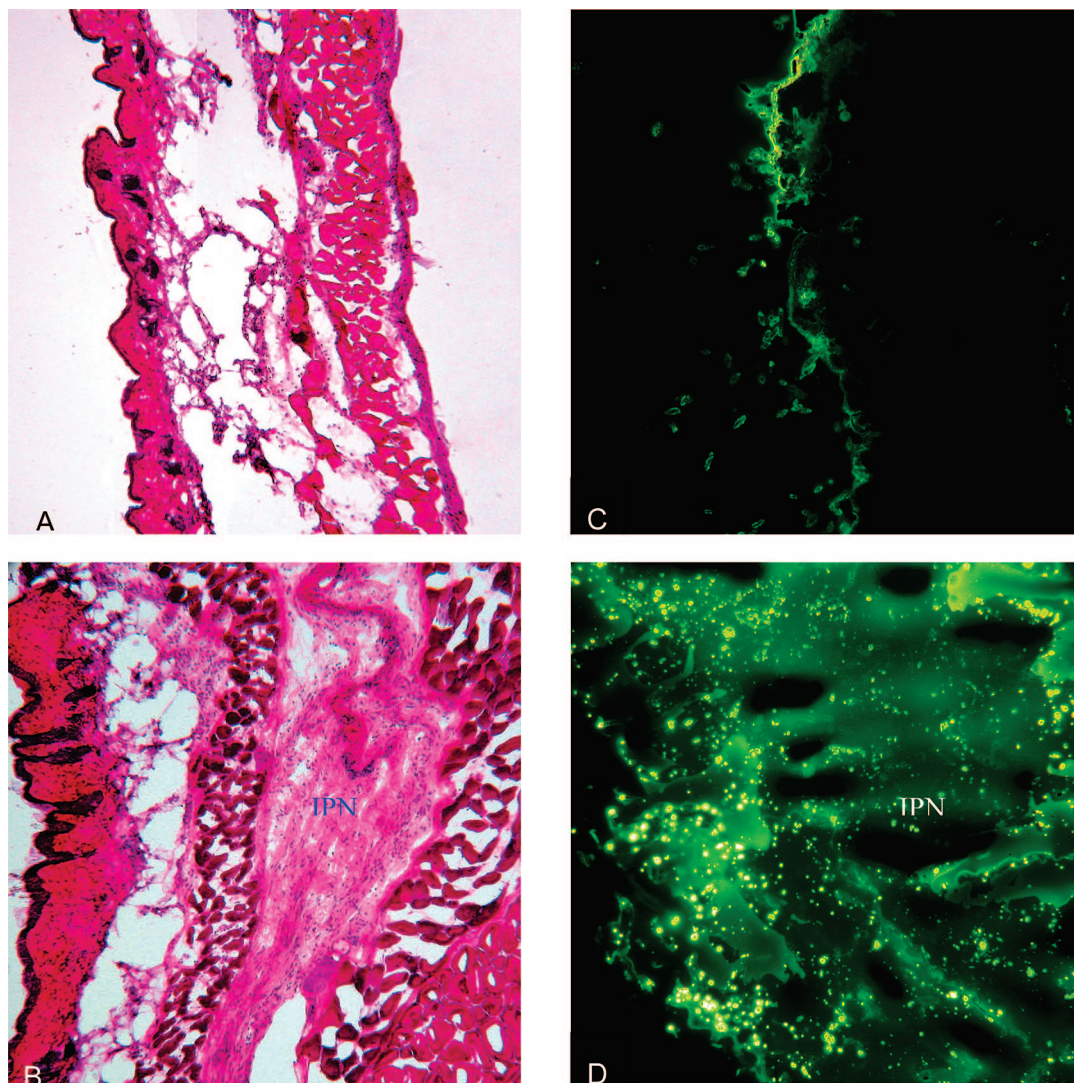


Figure 9. Biocompatibility and slow release property of IPN hydrogel were assessed in vivo. Balb/c mice were subcutaneously implanted with either fluorescein or fluorescein-loaded IPN gel. At 24 h post implantation, the animals were sacrificed and the implant-surrounding tissues were recovered for histological analyses. H&E stain shows that (A) fluorescein injection triggers minimal tissue response, whereas (B) hydrogel implant prompts mild inflammatory responses. On the other hand, fluorescence images of the tissues reveal that (C) a small amount of residual fluorescein was present in the fluorescein-injected tissue, although (D) a large amount of fluorescein still resides in the IPN hydrogel implanted tissue.

we find that most of the fluorescein dissipates from the implantation site, indicating a small retention rate of fluorescein in tissue (Figure 9c). On the other hand, a large amount of fluorescein is found in the microgel-implanted tissue, supporting that the presence of gelled microgel dispersion substantially reduces the diffusion and thus causes the slow release of fluorescein (Figure 9d). These results have shown that the PNIPAM-IPN-PAAC microgels do not adversely promote foreign body reactions in this acute implantation model. Equally important, our findings also support the slow release property of the IPN microgel dispersion that turns from a liquid to a gel as physiological temperature, as revealed by viscoelastic measurements in Figure 5.

Conclusion

PNIPAM-IPN-PAAC microgels were synthesized by first preparing PNIPAM microgels using a precipitation polymerization method and then using PNIPAM microgels as seeds to form an interpenetrating PAAC polymer network. The IPN microgels in water have an average hydrodynamic radius of

about 85 nm at 21 °C, measured by the dynamic light scattering method. The atomic force microscope image shows that the particles are much smaller with a diameter about 50 nm after they are dried but remain their spherical.

The storage and loss moduli G' and G'' of dispersions of IPN microgels are measured in the linear stress regime as a function of temperature at various polymer concentrations using a stress-controlled rheometer equipped with a solvent trap to prevent water evaporation. At a low polymer concentration of 1.5 wt %, G'' is always larger than G' over the entire temperature range studied. This indicates that the dispersion remains in a liquid state. However, as polymer concentration increases from 1.5 to 3.0 or to 6 wt %, there is an intercept between G' and G'' at 33 °C. Below the intercept temperature, G'' is larger than G' , but above this temperature, G' has much higher values than G'' , indicating the elastic response dominates. The frequency dependence of storage and loss moduli, G' and G'' , respectively, was determined in low-amplitude oscillatory shear experiments for IPN microgel dispersions. For dispersions with high polymer concentration (3.0 and 6.0 wt %) and at high temperatures (34

and 37 °C), the samples behave as viscoelastic solids and the storage modulus is larger than the loss modulus over the entire frequency range. The gelation temperature is found to be 33 °C by measuring loss tangent at various frequencies as a function of temperature. Because PAAc within PNIPAM-IPN-PAAc microgels is a weak acid, the gelation of IPN microgel dispersions depends on pH value effect. At pH 2.5, the protonation of carboxylic group within PAAc weakens the ability to absorb water. When heated above the gelation temperature, IPN microgels flocculate by pumping a large amount of water from the gel. When the pH value was adjusted to neutral, deprotonation of $-\text{COOH}$ groups on PAAc breaks complex structures between PAAc and PNIPAM and makes the microgel keep water even above the gelation temperature.

Via an animal implantation model, the results showed that the gelation process does not adversely promote foreign body reactions. On the other hand, we find that the gelation procedure creates a diffusion barrier and thus leads to slow release as expected. It is supported by our findings that most of the fluorescein, injected alone, dissipates from the implantation site quickly, while a large amount of fluorescein remains in the microgel-implanted tissue. The temperature-dependent gelation properties are proved to be useful for loading a variety of drugs and proteins at room temperature and slowly releasing the loaded agents at body temperature. These findings may lead to the development of novel slow release devices with improved safety and efficacy.

Acknowledgment. This work is supported by the National Science Foundation under grant no. DMR-0507208 (Z.H.), Texas Advanced Research Program (Z.H. and L.T.), and the National Institutes of Health grant GM074021 (L.T.).

References and Notes

- (1) Schild, H. G. *Prog. Polym. Sci.* **1992**, *17*, 163.
- (2) Pelton, R. H.; Chibante, P. *Colloids Surf.* **1986**, *20*, 247.
- (3) Hirotsu, Y.; Hirokawa, T.; Tanaka, T. *J. Chem. Phys.* **1987**, *87*, 1392.
- (4) Hoffman, A. S. *J. Controlled Release* **1987**, *6*, 297.
- (5) Yin, X.; Hoffman, A. S.; Stayton, P. S. *Biomacromolecules* **2006**, *7*, 1381–1385.
- (6) Han, C. K.; Bae, Y. H. *Polymer* **1998**, *39*, 2809.
- (7) Stile, R. A.; Healy, K. E. *Biomacromolecules* **2002**, *3*, 591–600.
- (8) Matsudo, T.; Ogawa, K.; Kokufuta, E. *Biomacromolecules* **2003**, *4*, 728–735.
- (9) Hu, Z. B.; Xia, X. H. *Adv. Mater.* **2004**, *16*, 305–308.
- (10) Xia, X. H.; Hu, Z. B. *Langmuir*, **2004**, *20*, 2094–2098.
- (11) Xia, X. H.; Hu, Z. B.; Marquez, M. J. *Controlled Release* **2005**, *103*, 21.
- (12) Hu, Z. B.; Xia, X. H.; Marques, M.; Weng, H.; Tang, L. P. *Macromol. Symp.* **2005**, *227* (Biological and Synthetic Polymer Networks and Gels), 275.
- (13) Guenet, J. M. *Thermoreversible Gelation of Polymers and Biopolymers*; Academic Press: London, 1992.
- (14) Franz, G. *Adv. Polym. Sci.* **1986**, *76*, 1.
- (15) Alexandridis, P.; Hatton, T. A. *Colloids Surf. A* **1995**, *96*, 1.
- (16) Jeong, B.; Kim, S. W.; Bae, Y. H. *Adv. Drug Delivery Rev.* **2002**, *54*, 37.
- (17) Chenite, A.; Chaput, C.; Wang, D.; Combes, C.; Buschmann, M. D.; Hoemann, C. D.; Leroux, J. C.; Atkinson, B. L.; Selmani, F. A. *Biomaterials* **2000**, *21*, 2155.
- (18) Silioc, C.; Maleki, A.; Zhu, K. Z.; Kjaniksen, A. L.; Nystrom, B. *Biomacromolecules* **2007**, *8*, 719–728.
- (19) Senff, H.; Richtering, W. *Langmuir*, **1999**, *15*, 102–106.
- (20) Zhao, Y.; Cao, Y.; Yang, Y. I.; Wu, C. *Macromolecules* **2003**, *36*, 855–859.
- (21) Cho, J.; Heuzey, M. C.; Begin, A.; Carreau, P. J. *Biomacromolecules* **2005**, *6*, 3267–3275.
- (22) Amin, S.; Kermis, T. W.; van Zanten, R. M.; Dees, S. J.; van Zanten, J. H. *Langmuir*, **2001**, *17*, 805–8061.
- (23) Seetapan, N.; Maingam, K.; Plucktaveesak, N.; Sirivat, A. *Rheol. Acta* **2005**, *45*.
- (24) Winter, H. H.; Chambon, F. *J. Rheol.* **1986**, *30*, 367.
- (25) Nordby, M. H.; Kjoniksen, A.-L.; Nystrom, B.; Roots, J. *Biomacromolecules* **2003**, *4*, 337–343.
- (26) Benec, L. S.; Snowden, M. J.; Chowdhry, B. Z. *Langmuir* **2002**, *18*, 6025–6030.
- (27) Weng, H.; Zhou, J.; Tang, L.; Hu, Z. *J. Biomater. Sci., Polym. Ed.* **2004**, *15*, 1167.

BM700918D